Modelling Simul. Mater. Sci. Eng. 3 (1995) 753–770. Printed in the UK

[redacted]

the Ag–Au system

Z W Lu†, Barry M Klein† and Alex Zunger‡

† Department of Physics, University of California, Davis, CA 95616, USA

atom, and (2) a set of interaction energies $\{J_\Gamma\}$ among the various sites belonging to a

expansion techniques [1, 27–30]

Figure 1. Geometric figures used in our cluster expansion. The expansion includes pair figures, three-body figures, and four-body figures. See table 3 for the definition of the figure coordinates.

many-body terms). We determine the N_J interaction parameters $\{J_F\}$ by mapping N_σ directly calculated $\Delta E_{\text{direct}}(\sigma)$ values onto $\Delta E_{\text{CE}}(\sigma)$ of equation (3) through a least-squares fitting procedure, i.e. by minimizing

$$\sum_{\sigma_s}^{N_\sigma} [\Delta E_{\text{direct}}(\sigma_s) - \Delta E_{\text{CE}}(\sigma_s)]^2 = \min \tag{4}$$

with respect to J_F. Convergence is tested by applying equation (3) to a set of structures $\{\sigma_s\}$ *not used in constructing* the cluster expansion for equation (4). We then

exchange–correlation potential (Wigner form) [59] used in [3]. We have calculated the excess total energies $\Delta E_{\text{direct}}(\sigma, V)$ of equation (2) for $N_\sigma = 32$ ordered structures $\{\sigma\}$ involving a small number of atoms in the unit cell (up to 8 atoms/cell) [5]. Figure 2 shows

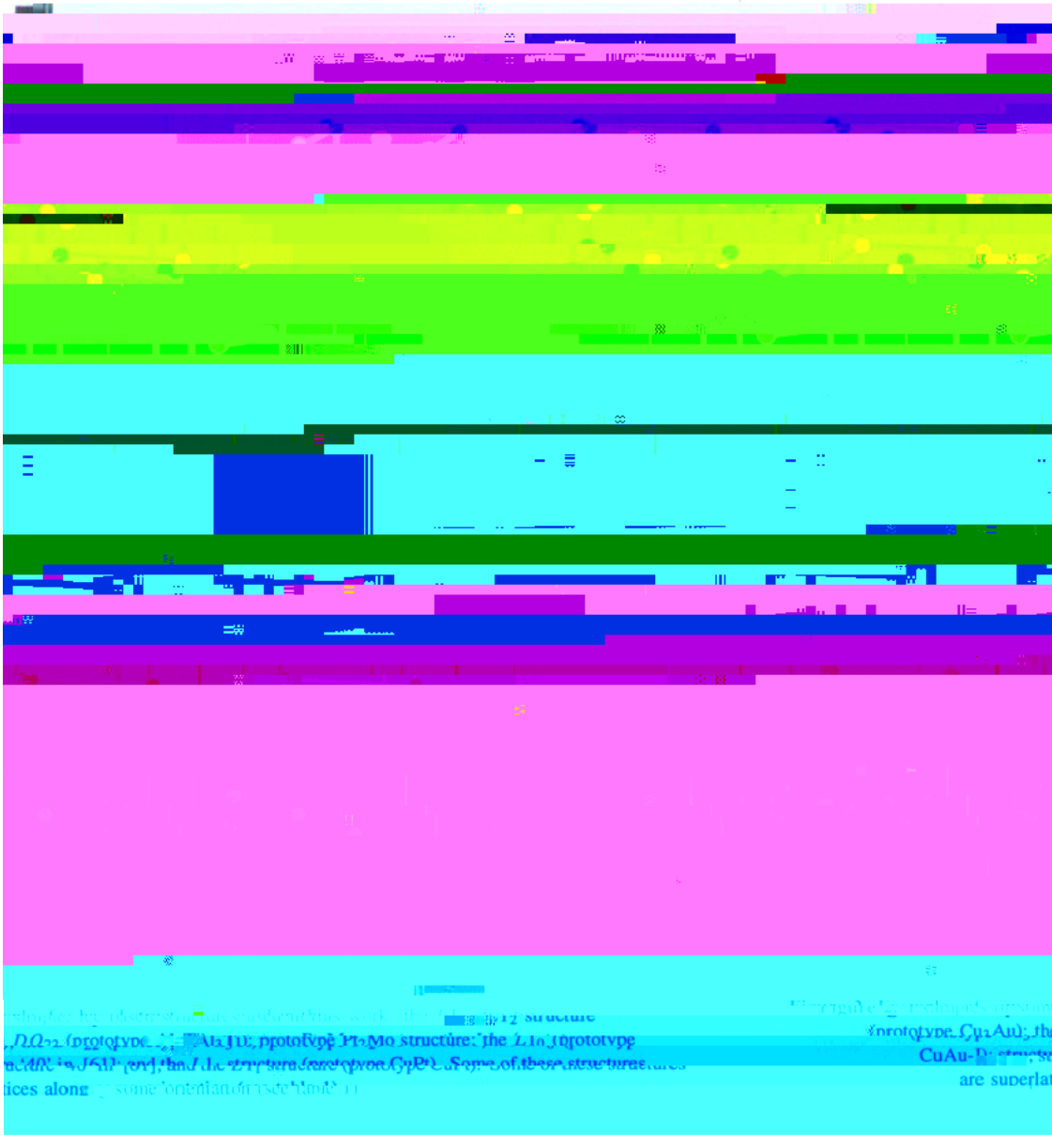

…simple fcc-based structures used in this work: the … $D0_{22}$ (prototype Al_3Ti); prototype Pt_2Mo structure; the $L1_0$ (prototype … (prototype Cu_3Au); the CuAu-… structure … 'A0' in [61]; and the $L1_1$ structure (prototype CuPt). Some of these structures are superlattices along some orientation (see table 1).

… examples of some simple fcc-based ordered structures used in our calculations. Table 1 and its caption define these structures. Most of these structures can be described as … period A_mB_n superlattices along some orientation as shown in figure 2 and table 1. The calculations for ordered compounds are all carried out at the average cubic … lattice relaxation on ΔH are small here (e.g., for A… Au … relaxation lowers the energy of the … Au system relaxation lowers the energy of the $L1_0$ structure by ~ 15 meV/atom). To obtain highly precise results we use a k-point sampling scheme that is geometrically equivalent …

Table 1. The directly calculated LAPW excess energies $\Delta E_{\text{direct}}(\sigma)$ (error $\sim \pm 2$ meV/atom) (equation (2)), the cluster-expanded energy $\Delta E_{\text{CE}}(\sigma)$ (equation (3)), and the prediction error

Table 2. This table illustrates the effects of k-point sampling on the calculated ΔE_{direct} (in meV/atom) of some ordered compounds. The structures are defined in table 1. We have

(AB). Using this original Connolly–Williams procedure, we obtained an average prediction error of $\delta_{PE} = 1.6$ meV/atom and a maximum prediction error of 4.4 meV/atom for 27 other structures that are not used in obtaining the interaction J values. The prediction errors for some specific structures are unsatisfactory. For example δ_{PE} are 4.4, 2.4, 3.0, 2.6 meV/atom, for structures '40', $\gamma 2$, DO_{22} ($AgAu_3$), and W3, respectively (larger than the estimated error of direct LDA calculation of 2 meV/atom). The large error for '40' and DO_{22} is because the Connolly–Williams set of interactions creates a spurious degeneracy

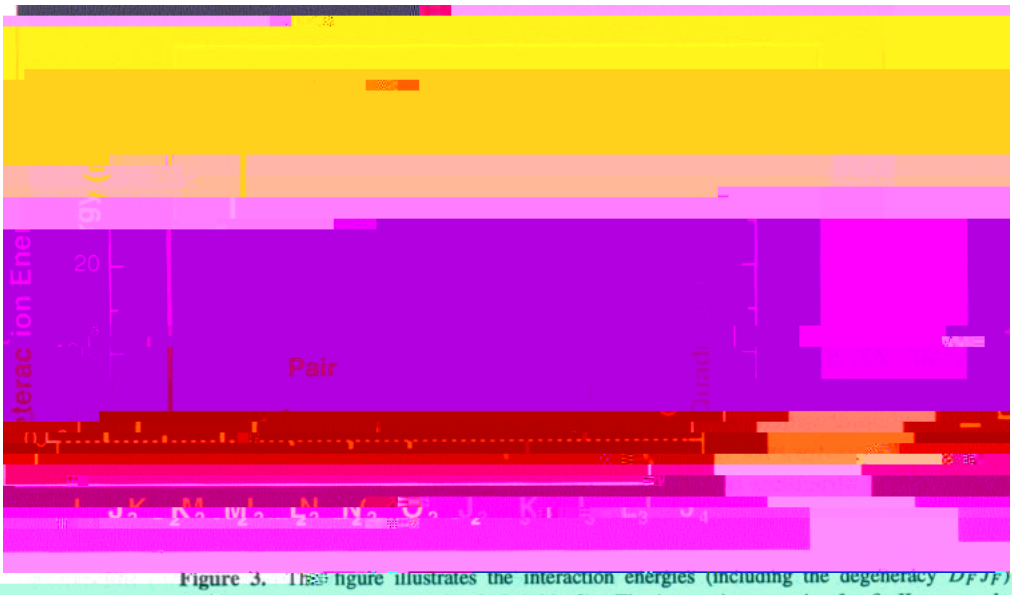

Figure 3. The figure illustrates the interaction energies (including the degeneracy $D_F J_F$) used in this work (figure 1) for fit I (table 3). The interaction energies for fit II are nearly indistinguishable on this scale. Note that the nearest-neighbor pair interaction J_2 is dominant.

Table 2. Geometrical definition of the 'figures' F used in our cluster expansion in terms of the

Cluster type	Designation for figure	Vertices
Triplets	J_3	(000)(110)(101)

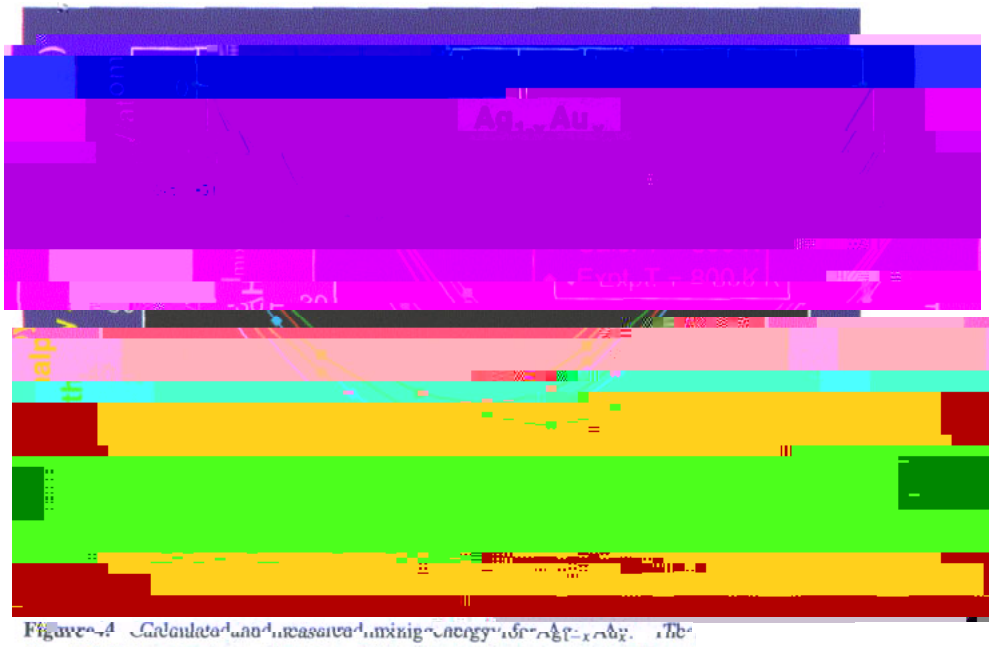

Figure 4. Calculated and measured mixing energy for $Ag_{1-x}Au_x$. The $T = 800$ K, lozenges) are cited from [23]. We give the calculated values

Table 4. The experimental [23] and calculated (fit I) $Ag_{1-x}Au_x$ mixing enthalpy ΔH_{mix} (meV/atom) using (i) Monte Carlo simulation at $T = 800$ K (including the short-range order effects and (ii) equation (6) corresponding to the completely ordered alloy ($\Delta H(x, T \to \infty)$).

x	ΔH_{mix}^{exp}	$\Delta H(x, T = 800\ \mathrm{K})$ Monte Carlo $T = 800$ K	$\Delta H(x, T \to \infty)$ Calc. (equation (6)) $T = \infty$
0.0	0.0	0.0	0.0
0.3	0.3	0.3	0.3

Table 5. The order–disorder phase transition temperatures T_c for $Ag_{1-x}Au_x$ alloys at $x = \frac{1}{4}$, $\frac{1}{2}$, and $\frac{3}{4}$. The calculated results were obtained using N_J interactions, solving the ensuing Ising model with the Monte Carlo (MC) method or with the cluster variation method (CVM). The 'measured' data were obtained by (i) using an inverse Monte Carlo method to extract three composition-dependent effective pair interactions from the short-range order data of the Georgopoulos–Cohen (GC) and Borier–Sparks (BS) analyses and (ii) subjecting the these effective interactions to a direct Monte Carlo simulation.

		Ag_3Au $L1_2$	AgAu $L1_0$	$AgAu_3$ $L1_2$
Calculated (K)				
Present, fit I	$N_J = 12$; MC	155	210	225
Wei *et al*[a]	$N_J = 5$; CVM	120	240	200
Mohri *et al*[b]	$N_J = 5$; CVM	152	177	183
'Measured' (K)				
Schönfeld *et al* (BS)[c]	$N_J = 3$; MC	115	115	155
Schönfeld *et al* (GC)[d]	$N_J = 3$; MC	165	165	210
Norman and Warren[e]		90		
Ziesemer[f]			168	

Figure 5. (a) Calculated SRO diffuse-scattering intensity for $Ag_{1-x}Au_x$ ($x = 0.51$) using Connolly–Williams set of nearest-neighbor $N_J = 5$ interaction energies, (b) calculated SRO map using our set of $N_J = 12$ interaction energies, and (c) experimental diffuse-scattering intensity due to chemical SRO, $\alpha(\mathbf{k}, T/K)$ for $Ag_{0.477}Au_{0.523}$, which were Fourier-synthesized using $N_R = 13$ real-space $\alpha(\mathbf{R})$. (Reproduced from [...] for [illegible] experimental

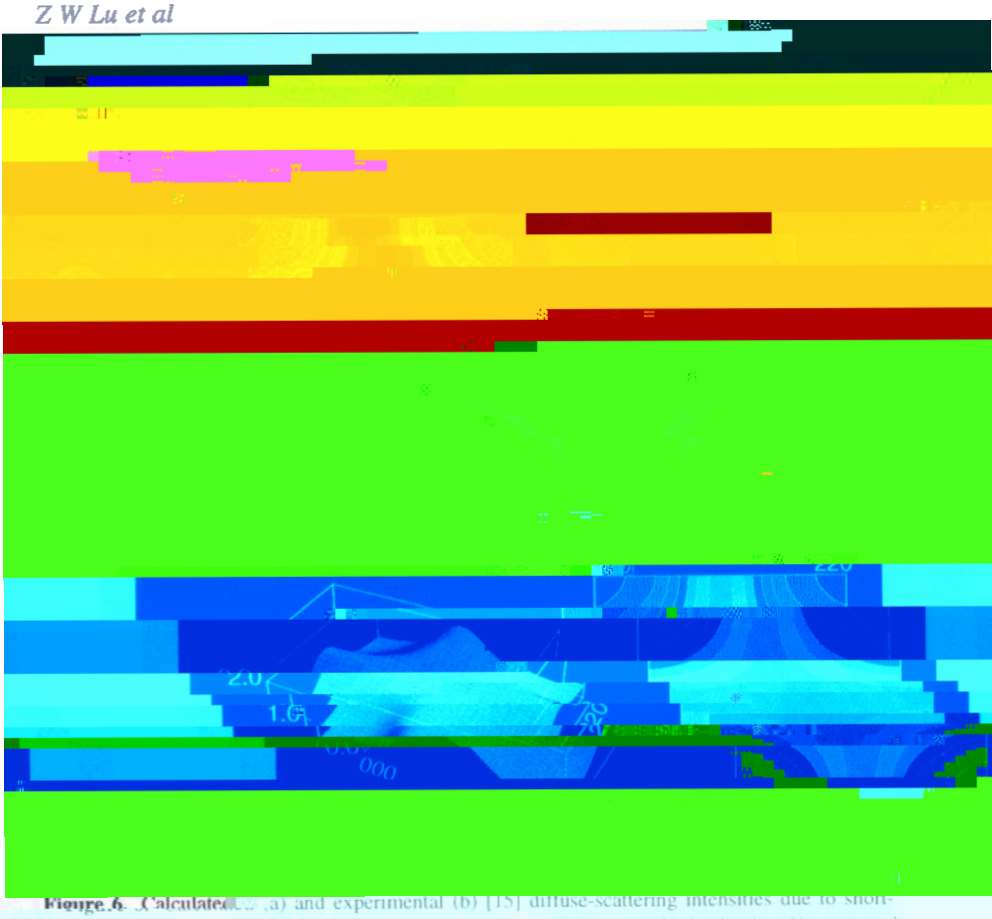

Figure 6. Calculated (a) and experimental (b) [15] diffuse-scattering intensities due to short-range order in Cu$_{0.75}$Au$_{0.25}$ alloy. Fourier synthesized using $\alpha(\kappa_{lmn})$ for the real space $\alpha(\kappa_{lmn})$ (including $\alpha(\kappa_{000}) \equiv 1$ for both experiment and theory). The calculation was done at $T = 600$ K, while the experiment was performed on a sample that was homogenized at $T = 1173$ K and later aged at $T = 515$ K.

mixing

values with experiment [23]. The agreement is excellent. Note that the finite-temperature

and by Ackland and Vitek [25] and the semiempirical method by Bozzolo and coworkers

order map correctly reproduce the shape and composition dependence of the short-range

3.4. $T = 0$ ground state structures

The ground state problem can be solved using the linear programming method [61, 62]. For

alloys, the most complete searches for the ground state were given by Kan

Figure 7. Calculated (a) and experimental (b) [15] diffuse-scattering intensities due to short-range order $\alpha(k, N_R)$ for $Ag_{0.750}Au_{0.250}$, which were Fourier synthesized using $N_R = 210$ real-space pairs in $R(N_{max})$ (including $\alpha(R_{max}) = 1$ for both experiment and theory). The calculation was done at $T = 600$ K.

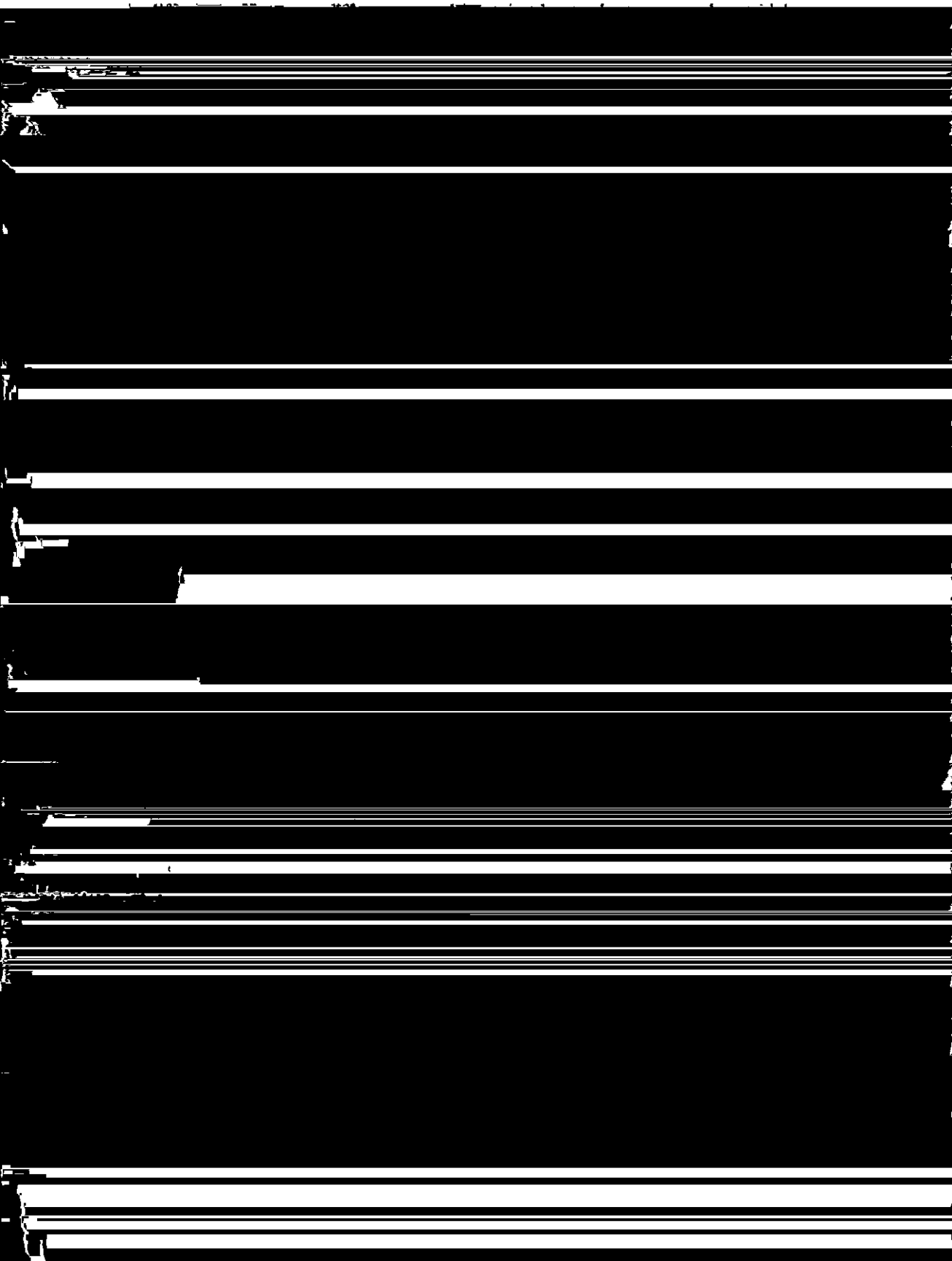

difference at $x = 0.5$ is -4.4 meV/atom, correlating with a fairly pronounced peak at the X point for $\alpha_{\mathrm{SRO}}(k)$ at $x = 0.523$.

4. Conclusions

We have demonstrated here that accurate alloy properties can be obtained from *ab initio*

[26] Bozzolo G, Ferrante J and Smith J R 1992 *Phys. Rev.* B **45** 493
[27] Terakura K, Oguchi T, Mohri T and Watanabe K 1987 *Phys. Rev.* B **35** 2169–73
[28] Mohri T, Terakura K, Oguchi T and Wantanabe K 1988 *Acta Metall. Mater.* **36** 547–53
[29] Mohri T, Terakura K, Takizawa S and Sanchez J M 1991 *Acta Metall. Mater.* **39** 493–501
[30] Mohri T, Takizawa S and Terakura K 1992 *J. Phys.: Condens. Matter* **5** 1473–80